GOES EUVS Measurements

Janet Machol, NOAA National Centers for Environmental Information (NCEI) and U. of Colorado, CIRES
Rodney Viereck, NOAA Space Weather Prediction Center (SWPC)
Andrew Jones, U. of Colorado, LASP

8 November 2016, Version 3.1.3

Caution: For version 2 data (Channels A and B), the 1-min average timestamps are *incorrectly* offset by about 11 s. (See Section 3.1.2.)

Version	Date	Change description	author
3.1.3	30 Sep 2016	added a ref to Viereck, fixed path format, changed main directory GOES Channel E data revised as follows: Data goes to summer 2016. Flags have been created for pre-2010 and revised for post 2010. The fit is to SORCE SOLSTICE v15. A time stamp error has been fixed.	
3.1.2	30 Sep 2015	Fixed equation in Figure 13 caption. Revised directory structure for data. For Channel E, raw data - flags created for pre-2011 data and extended for later data. - flag 1048576 (in-flight calibration) no longer in raw data. - bad data is marked better with flags For Channel E, processed data (version 4) - flag 9 option removed from 1 minute data. - Daily averages exclude +/- 4 hours around midnight. - Fit is to SORCE SOLSTICE v 15. - fixed 12 s time stamp error in 1 min averaged files	Machol
3.1.1	12 Aug 2015	Fixed error in Equation 2.	Machol

3.1	4 March 2015	original	Machol

Contents

1. Summary

The geostationary orbiting GOES 13-15 satellites were launched in 2006, 2009, and 2010 respectively. They each carry an Extreme Ultraviolet Sensor (EUVS; Viereck et al., 2007; Evans et al, 2010) which measures the EUV in 5 bands (A-E) from about 5-127 nm as shown in Figure 1. The raw data is in counts with a 10.24 s sample rate and a requirement of <15% uncertainty. GOES 14 is unique in that it measures duplicate A and B bands (with the A' and B' channels) instead of C and D bands.

The raw data comes from the NOAA Space Weather Prediction Center (SWPC) and is further processed and archived by the NOAA National Centers for Environmental Information (NCEI). NCEI currently provides calibrated data for the A, B and E bands for all three satellites. Times of available GOES EUVS measurements are shown in Figure 2; so far, only Channel E is processed after mid-2014.

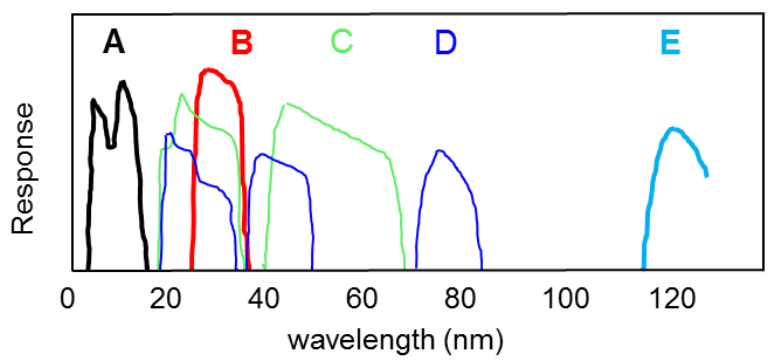

Figure 1. Wavelength responses of the GOES EUV sensors for the A-E bands.

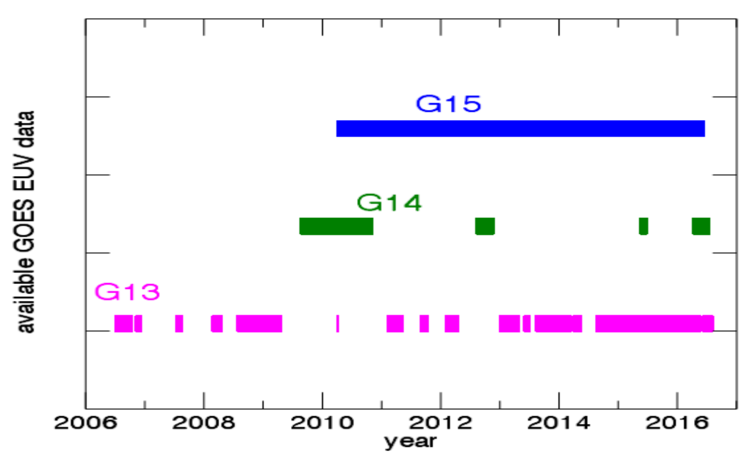

Figure 2. Available EUV measurements from GOES satellites. So far, only Channel E is processed since 2015.

The EUVS raw count data is converted into irradiances using measured detector response curves and quiet sun reference spectra. In general, measurements of the A and B bands agree well with other instruments and there has been no noticeable degradation. The E bands have noticeable degradation which varies between instruments. The Channel E data is scaled to the daily SORCE SOLSTICE [McClintock et al., 2005] Lyman-α values with an exponential function that simultaneously corrects for degradation and the absolute value. The residual from this scaling is a few percent or less, and so this process provides corrected 1 minute Lyman-α data which is based on daily Lyman-α from SOLSTICE. Figure 3 through Figure 5 show the measured irradiances for the A, B, and E bands.

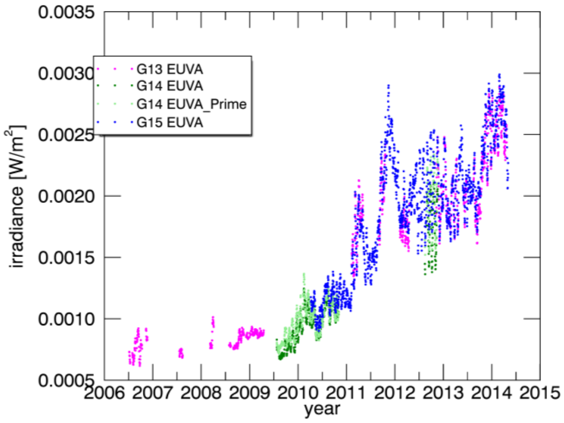

Figure 3. Irradiances for Channel A of GOES-13, -14 and -15. Irradiances for GOES-14 Channel A' are also shown.

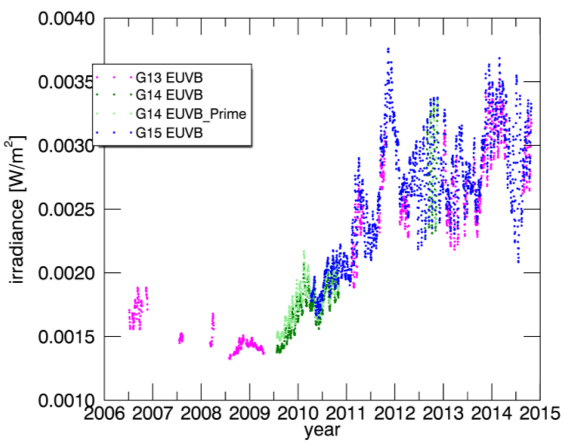

Figure 4. Irradiances for Channel B of GOES-13, -14 and -15. Irradiances for GOES-14 Channel B' are also shown.

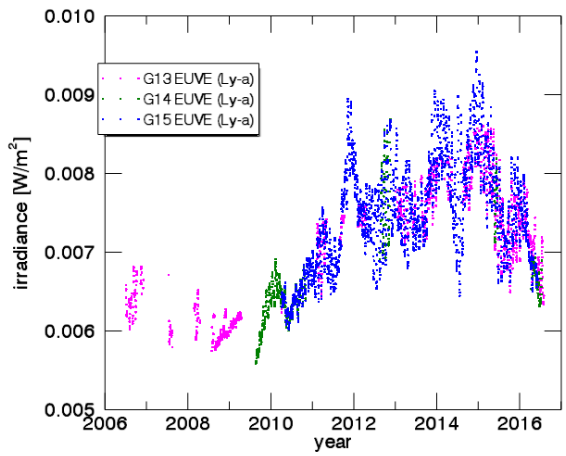

Figure 5. Daily irradiances from Channel E corrected to match the SORCE SOLSTICE Lyman-α band for GOES-13, -14 and -15 for version 4 data.

2. Data access

The NCEI archive provides raw (10.24 s) counts and flags, and calibrated ASCII data files with 1-min and daily averaged counts, irradiances and flags. Column and format information is in the file headers. The E channel files also contain 1-min and daily irradiances which have been adjusted to a 1-nm bandpass around the Lyman-α line and which are scaled to SORCE SOLSTICE. The data archive also includes annual "quick look" plots; An example plot is shown in Figure 6. Currently, version 2 data (Channels A and B) are available up to October 2014, while version 4 (Channel E) data is available through July 2016. Data processing and file production is not yet automated, but the dataset will be updated periodically. Automation will hopefully occur soon.

High cadence (10.24 s) irradiances can be created from the raw counts with the values with Equation 1 given in Section 3 in conjunction with the tables in Appendix A. For Channel E, the degradation equation (Eq. 2) will need to be applied as well. Count and irradiance data is not adjusted to 1 AU. However, correction files with daily 1 AU corrections are provided separately and the factors in them can be interpolated for use with the 10-s and 1 min data. The daily irradiance files contain a column with 1 AU correction factors.

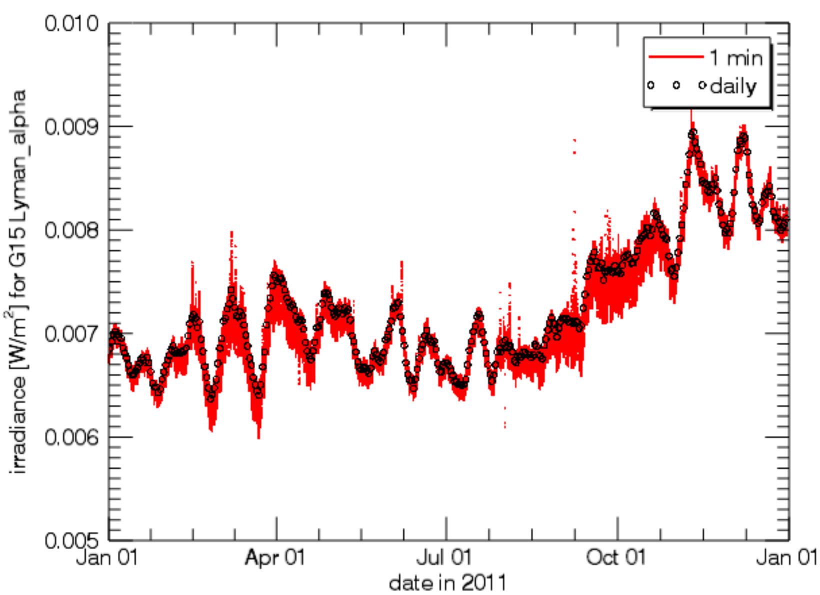

Figure 6. Irradiance plot with 1 min and daily averages for 2011 for GOES-13 Channel E data. Plots like these are available in archive.

2.1 Available files

The following archived files are available at the NCEI website. Variables are

nn	satellite
c	channel
x	data version; Table 1 lists the current data versions
yyyy	year of data

The **main data directory** is....

http://satdat.ngdc.noaa.gov/sem/goes/data/euvs/

Yearly files of calibrated counts and irradiances .../GOES_vx/G*nn*/

G*nn*_EUV*c*_*yyyy*_vx.txt	*1 minute data (counts, irradiances, and flags)*
G*nn*_EUV*c*_*yyyy*_daily_vx.txt	*daily data (counts, irradiances, and flags)*
G*nn*_EUV*c*_y_{start}_y_{end}_daily_vx.txt	*daily data combined for years* y_{start} *to* y_{end}

Raw data files with 10.24 s cadence counts .../raw_10s/ G*nn*/

G*nn*_EUV*c*_Cnts_*yyyy*.dat	*raw 10s counts*
G*nn*_EUVA_Corrected_Cnts_*yyyy*.dat	*10s counts corrected for heater noise; Channel A only*
G*nn*_EUV*c*_Flags_*yyyy*.dat	*flags for 10s data (improved)*
orig_G*nn*_EUV*c*_Flags_*yyyy*.dat	*original flags–use if improved flag files not available*

Plots .../plots_ vx/G*nn*/

G*nn*_EUV*c*_counts_yyyy_vx.png	*1 year plot of 1 minute and daily counts*
G*nn*_EUV*c*_irrad_yyyy_vx.png	*1 year plot of 1 minute and daily irradiances*

1 AU correction files .../AU_correction/

AU_correction_factor_daily.txt	*daily factors to convert data to 1AU, by doy*
AU_correction_factor_daily_2006_2020.txt	*daily factors to convert data to 1AU, by date*

Documentation http://ngdc.noaa.gov/stp/satellite/goes/doc/

GOES_NOP_EUV_readme.pdf	GOES *EUVS readme file*
GOES_XRS_readme.pdf	*GOES XRS readme file*

Table 1. Latest versions for processed GOES EUVS data.

sat ch	version	comments	latest data
15 A	2	corrected for heater noise	April 14
15 B	2		Oct 2014
15 E	4	uses temperature dependent background; scaled to SORCE SOLSTICE v15	Sep 2016
14 A, A'	2	corrected for heater noise	2012
14 B, B'	2		2012
14 E	4	scaling to SORCE SOLSTICE v15 (excluded anomalous times before Dec 2009 and in 2012); temperature dependent background	Sep 2016
13 A	2	corrected for heater noise	April 2014
13 B	2		Oct 2014
13 E	4	correction inadequate - data should not be used for now uses temperature dependent background; scaled to SORCE SOLSTICE v15	Sep 2016

3. Data calibration and processing

3.1 Calibration

Count data is converted to calibrated fluxes with the equation:

$$\text{EUV Channel Irradiance [W/m}^2\text{]} = ((\text{Counts} - B\ \text{[counts]}) * G\ \text{[A/count]} - V\ \text{[A]}) / C\ \text{[A/(W/m}^2\text{)]} \quad \text{(Eq. 1)}$$

where for each channel, *B* is the background, *G* is the gain, *V* is the visible light contamination, and *C* is a units conversion factor. The values for the *G* and *V* come from the GOES Data and Calibration Handbooks. The temperature-dependent background values, *B*, are really electronic offsets, and are determined from the measurements when the satellite is pointed away from the Sun. The conversion factors are determined from a convolution of the measured detector spectral responses with a quiet sun spectrum and change with solar activity level (Appendix B2). Calibration factors are given in the tables of Appendix A.

3.1.1 Raw data

The EUVS channels accumulate counts for 10.24 s. As shown in Figure 7, for Channels A and B, the time stamps occur 1.024 s after the end of the accumulation, while for Channels C-E, the time stamps occur 2.048 s after the end of the accumulation. The integration periods for different channels are not concurrent.

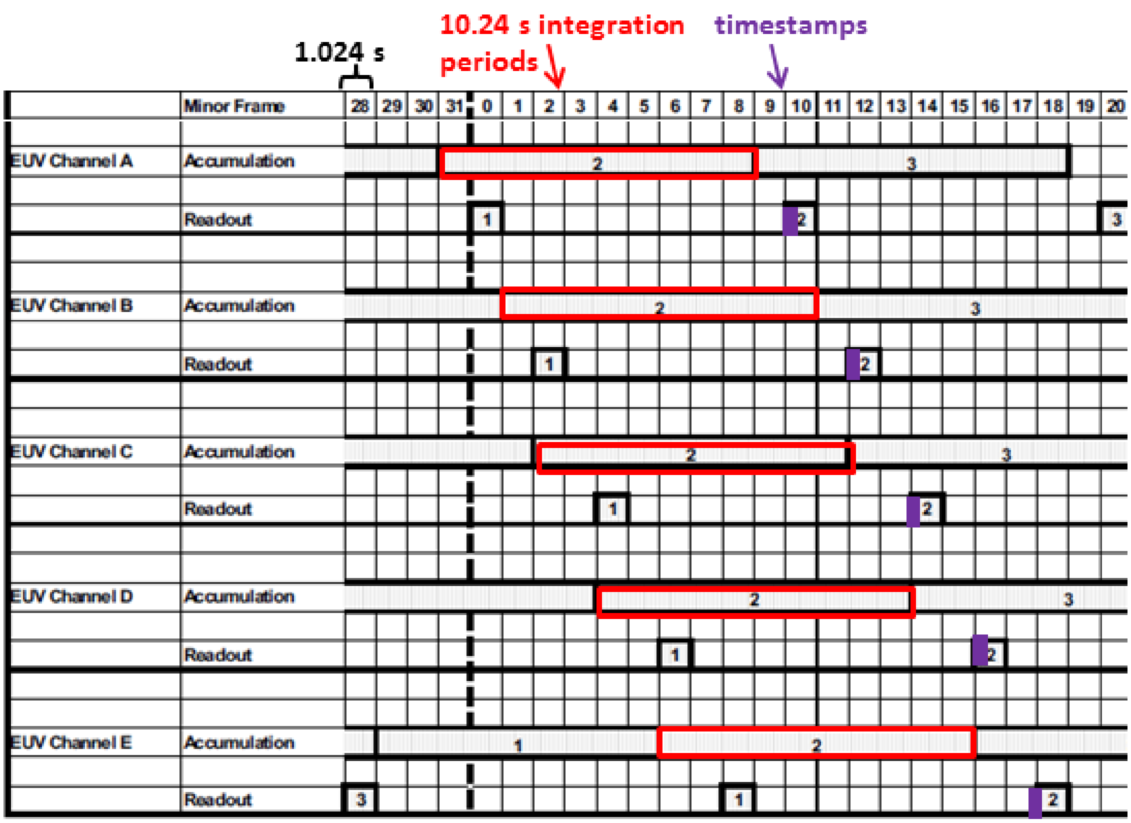

Figure 7. Sketch of EUVS instrument timing. Telemetry minor frames are 1.024 s. Integration is 10.24 s and timestamps occur 1.024 or 2.048 s after the end of the integration, depending on channel.

Table 2. For Channel E data, the flags have been revised in the NCEI processing, so that there are now flags before 2010, and better flag coverage for the later dates.

Table 2. Flags for 10-s count data. Real count values are denoted as *x*.

flag	definition	counts	note
0	no flag	*x*	
-99999	bad or missing data	-99999	
1048576	in-flight calibration (only 2009-2010)	*x*	*not in revised Ch E data*
2097152	off-pointed	*x*	
3145728	off-pointed and in-flight calibrations	*x*	
4194304	Sun is eclipsed by the Moon	*x*	
8388608	Sun is eclipsed by the Earth	*x*	
12582912	Sun is eclipsed by the Moon and the Earth	*x*	
14680064	Sun has unknown eclipsed (Moon or Earth)	*x*	

3.1.2 Averages of 1 minute

The 1-min averaged data is created from averages of the raw 10-s count data excluding spikes, dropouts, and other bad data. The A channel counts are also (partially) cleaned of noise from the Solar X-ray

Imager (SXI) heater as described in Appendix B2. The averaged irradiances are created from the averaged counts with Eq. 1.

The flags for the 1 minute data are shown in Table 3. The 'partial eclipse flag' is set for data near eclipse periods to indicate that the counts are reduced by thermal effects. The number of minutes of partial eclipse flags set on either side of an eclipse depends empirically on the eclipse duration. Partial eclipse flags are set for 8 mins before and 5 mins after eclipse periods longer than 30 mins, and for 12 mins before and 10 mins after eclipse periods shorter than 30 mins.

Each 10-s record with good data is averaged into the 1 min period in which its midpoint lies. Timestamps for 1-min data are in middle of the period. **The version 2 data (channels A and B) has timestamps for the 1 minute averaged data: the times stamps are late by 11-12 s. Tthis error is because the 10-s timestamp offsets were incorrectly assumed to be at the start of the accumulations instead of 1-2 s beyond the ends.** These timestamps are correct in the version 4 data for Channel E. The raw data spacing is 10.24 s, and so 97% of the 1-min averages contain 5 or 6 raw records. About 3% of the 1-min records have no data (flags 5, 8 or -999).

Table 3. Flags and values in 1-min averaged data. Actual counts or irradiance values are denoted as *x*.

flag	definition	flags in 10-s source records	counts	irradiance
0	no flag	all data in average had flag=0 and no partial eclipse	*x*	*x*
1	possible bad data	Used in GOES14 Chan E before 1 December 2010 when there is a different degradation rate based on fit to SOLSTICE Lyman-α data; included in daily values	*x*	*x*
2	partial eclipse	Flag set to 0 in 1-minute average routine. Later analysis adds partial eclipse flags near times with eclipses.	*x*	*x*
5	eclipse	At least one eclipse flag (flag >4,000,000) and no off-point or calibration flags.	-999	-999.0
8	off-pointed or in-flight calibrations	At least one off-point or calibration flag (1,000,000 < flag < 4,000,000)	-999	-999.0
-999	bad or missing data	all flags were -99999	-999	-999.0

3.1.3 Daily averages

The daily averages are based on averages of the 1 min data. There are only three flags options for the daily averages as shown in Table 4. Timestamps are the middle of the integrated period.

For the channel E data, the daily average excludes times within ±4 h of local midnight, in order to exclude dips near midnight due to geocoronal hydrogen absorption. The dips range from about 0.3 to 6% and are largest around the equinoxes. Excluding the dips results in about a 1% change in the daily averages.

Table 4. Flags and values in daily averaged data. Actual counts or irradiance values are denoted as *x*.

flag	definition	flags in 10-s source records	counts	irradiance
0	no flag	all data in average had a 1 min flag of 0	*x*	*x*
1	possible bad data	all data in average had 1 min flags of 0 or 1	*x*	*x*
-999	bad or missing data	no average because there were no 1 min flags of 0 or 1	-999	-999.0

3.2 Channel E degradation and Lyman-α

The GOES Channel E data is converted to a 1 nm band around the Lyman-α line at 121.6 nm. Based on the LASP WHI quiet sun reference spectrum [Woods et al., 2009], about 88% of the full channel irradiance is contained in the 1-nm band (Table 7 in Appendix A). To correct for degradation in the E channel, the GOES data is scaled to SORCE SOLSTICE Lyman-α measurements. The ratio of the daily averaged GOES Lyman-α to the daily SOLSTICE Lyman-α is fit for version 4 data with the function:

$$y(t) = A_0 \exp[A_1 \cdot (t - t_0)] + A_2 \cdot (t - t_0) + A_3 \qquad \text{(Eq. 2)}$$

The daily and one minute GOES Lyman-α data is then divided by this function which scales the data to SOLSTICE and corrects for degradation. The amount of degradation for Channel E as a function of year is given in Table 5. The factors for the scaling function are given in Table 13 in Appendix A.

Table 5. Amount of degradation for Channel E after a given number of years from launch date based on the fit parameters in Error! Reference source not found.**.**

	after: 1 year	2 years	5 years	10 years
GOES13	1%	1%	6%	23%
GOES14	15%	17%	20%	23%
GOES15	10%	17%	30%	46%

4. Future improvements to the data

There are number of refinements that should be done on the EUVS data processing. These include:

- Automate file creation.
- Correct time stamps in 1 minute averaged data for Channels A and B.
- Correct for heater spikes in counts from Channels A and B.
- Determine how best to apply reference spectra that vary with solar activity.
- Determine best way to combine the duplicate A and B channels on GOES 14 to get cleaner data.
- Process Channels C and D on GOES 13 and 15.
- Improve correction for GOES-13 Channel E data.
- Create composites with data from all three satellites.

References

Evans, J.S., Strickland, D.J., Woo, W.K., and D. R. McMullin, S. P. Plunkett, R. A. Viereck, S. M. Hill, T. N. Woods, F. G. Eparvier (2010), Sol Phys 262: 71, doi:10.1007/s11207-009-9491-x.

McClintock, William E., M. Snow and T. N. Woods, (2005), Solar Phys. 230, doi:10.1007/s11207-005-1585-5.

Meier, R. R., H. P. Warren, A. C. Nicholas, J. Bishop, J. D. Huba, D. P. Drob, J. L. Lean, J. M. Picone, J. T. Mariska, G. Joyce, D. L. Judge, S. E. Thonnard, K. F. Dymond, and S. A. Budzien (2002), Ionospheric and dayglow responses to the radiative phase of the Bastille Day flare, Geophys. Res. Lett., 29, doi:10.1029/2001GL013956.

Viereck, R., F. Hanser, J. Wise, S. Guha, A. Jones, D. McMullin, S. Plunket, D. Strickland, S. Evans (2007), "Solar extreme ultraviolet irradiance observations from GOES: design characteristics and initial performance", Proc. SPIE 6689, Solar Physics and Space Weather Instrumentation II, 66890K, doi:10.1117/12.734886.

Warren, H.P.(2005), Astrophys. J. Suppl. Ser. 157, 147. doi:10.1086/427171.

Woods, T. N., P. C. Chamberlin, J. W. Harder, R. Hock, M. Snow, F. G. Eparvier, J. Fontenla, W. E. McClintock, and E. C. Richard (2009), Solar Irradiance Reference Spectra (SIRS) for the 2008 Whole Heliosphere Interval (WHI), Geophys. Res. Lett., 36, doi:10.1029/2008GL036373.

Data Sources

LASP WHI spectra (http://lasp.colorado.edu/lisird/whi_ref_spectra/

Contacts

Please contact janet.machol@noaa.gov for comments and questions regarding the archived GOES EUVS data or this document, or if you wish to be added to a mailing list for updates on the GOES EUVS data set.

Appendix A. Calibration Tables

The conversion from count rates into irradiances is done with Eq. 1 and the values in tables in Appendices A1, A2, and A3. The scale factors in the tables can be used to scale the bandpasses of the GOES channels to match the bandpasses of other instruments. **Error! Reference source not found.** rovides the fit parameters to correct for degradation in the Channel E Lyman-α data for all three satellites.

A1. Tables for GOES 13

Table 6. Correction factors for GOES 13. Gain and background values are for a telescope temperature of 12C. For Channel E, the background used for flux calculation is a function of temperature as given in

Table 12.

channel	Background [counts]	Gain [A/counts]	Visible Light Contamination [A]	bandpass [nm]
A	25198	1.91E-15	2.13E-14	2.8-20.6
B	15970	1.89E-15	1.21E-14	2.8-36.4
C	16229	1.90E-15	4.79E-14	-
D	24387	1.89E-15	1.20E-15	-
E	25096	1.90E-15	1.32E-12	113.5-132.8

Table 7. Flux conversion factors, *C*, for GOES-13 channels for solar minimum and maximum conditions. Also shown are scale factors, *f*, to match the bandpasses of other instruments.

channel	solar activity	C[A/(W/m^2)]	f_{EVE} 5-15 nm	f_{EVE} 25-34 nm	f_{SOHO} 26-34 nm	$f_{Lyman\text{-}\alpha}$ 121.0-121.9 nm
A	minimum	8.918e-10	0.21	-	-	-
A	maximum	8.065e-10	0.19	-	-	-
B	minimum	6.615e-09	-	0.406	0.368	-
B	maximum	6.034e-09	-	0.381	0.335	-
E	minimum	2.612E-09	-	-	-	0.884

A2. Tables for GOES 14

Table 8. Correction factors for GOES 14. Gain and background values are for a telescope temperature of 12C. For Channel E, the background used for flux calculation is a function of temperature as discussed in Section A4.

Table 12.

channel	Background [counts]	Gain [A/counts]	Visible Light Contamination [A]	bandpass [nm]
A	26571	1.92E-15	1.04E-14	2.8-19.0
B(A')	23948	1.93E-15	7.18E-14	2.8-19.0
C (B)	14207	1.93E-15	2.96E-13	6.0-36.6
D (B')	24856	1.95E-15	5.47E-14	6.0-36.6
E	25188	1.94E-15	2.49E-12	113.7-135.9

Table 9. Flux conversion factors, *C*, for GOES-14 channels for solar minimum and maximum conditions. Also shown are scale factors, *f*, to match the bandpasses of other instruments.

channel	solar activity	C[A/(W/m^2]	f_{EVE} 5-15 nm	f_{EVE} 25-34 nm	f_{SOHO} 26-34 nm	$f_{Lyman-\alpha}$ 121.0-121.9 nm
A	minimum	8.718e-10	0.256	-	-	-
A	maximum	8.691e-10	0.248	-	-	-
A'	minimum	8.744e-10	0.256	-	-	-
A'	maximum	8.628e-10	0.248	-	-	-
B	minimum	4.841e-09	-	0.424	0.385	-
B	maximum	4.441e-09	-	0.406	0.357	-
E	minimum	2.630e-09	-	-	-	0.855

A3. Tables for GOES 15

Table 10. Correction factors for GOES 15. Gain and background values are for a telescope temperature of 12C. For Channel E, the background used for flux calculation is a function of temperature as given in

Table 12.

channel	Background [counts]	Gain [A/counts]	Visible Light Contamination [A]	bandpass [nm]
A	49454	1.91E-15	1.78E-14	3.6-20.8
B	49797	1.90E-15	2.71E-14	3.6-38.5
C	55451	1.90E-15	2.03E-15	-
D	51218	1.90E-15	4.37E-14	-
E	40947	1.90E-15	2.23E-12	116.3-132.4

Table 11. Flux conversion factors, *C*, for GOES-15 channels for solar minimum and maximum conditions. Also shown are scale factors, *f*, to match the bandpasses of other instruments.

channel	solar activity	C[A/(W/m^2]	f_{EVE} 5-15 nm	f_{EVE} 25-34 nm	f_{SOHO} 26-34 nm	$f_{Lyman-\alpha}$ 121.0-121.9 nm
A	minimum	1.100e-09	0.213	-	-	-
A	maximum	1.006e-09	0.193	-	-	-
B	minimum	3.786e-09	-	0.399	0.363	-
B	maximum	3.594e-09	-	0.379	0.333	-
E	minimum	2.348e-09	-	-	-	0.884

A4. Background counts as a function of temperature

For Channel E, the background counts are a function of the Imager Mounting Platform (IMP) temperature which is usually in the range of 4-6 C. Linear functions for GOES 13 and 15 are found by comparing the background to the temperature when the satellite points away from the sun, time periods known as 'offpoints. For this calibration, the IMP temperature measurement was chosen instead of the SXI temperature measurement, which has better resolution, but is further away, and the EUV temperature measurement (range of 11-13 C) which was less well correlated to the background counts.

Table 12. Coefficients A, B, and C for determination of background count, $B(T) = (A + B*T + C*T^2) *D$ for IMP temperature (T). Typical temperatures are 4-6C.

satellite	A	B	C	D
13	25326.335	-41.787008	0	1
14	40348.1	37.4596	1.62123	0.621658
15	40638.198	77.106458	0	1

A5. Lyman-α fit parameters

Table 13. Version 4 fit parameters for the degradation function $y(t)=A_0 \exp[A_1(t- t_0)] + A_2(t- t0) + A_3$ for time, *t*, in units of Julian Day. The Lyman-α data from Channel E is corrected for degradation and scaled to SOLSTICE by dividing by this function. The fit for GOES14 starts on 1 Dec 2009 and excludes the data in 2012. Values in blue are changed in version 3 from previous version 2. *We do not recommend using the GOES13 Channel E data until we determine more corrections to it.

	A_0	A_1	A_2	A_3	t_0 [Julian Day]
GOES13*	-10.506987	-6.5582174e-005	-0.00068685569	11.635565	2453857
GOES14	0.20419478	-0.0070176921	-2.7219186e-005	1.0905254	2454984
GOES15	0.20327572	-0.0016817982	-0.00011181107	1.1090724	2455257

Appendix B. Processing Procedure

B1. Channel A temperature correction

The GOES NOP EUV-A Channel data has noise spikes that are correlated with the Imager Mounting Platform (IMP) heater. The heater keeps the IMP at a stable temperature and has fixed set points that are not controllable from the ground. During the coldest parts of the GOES season (summer), the heaters cycle about every 10 – 50 minutes. During the warmest parts of the GOES season (winter) the heaters are sometimes not required at all and may stay off for weeks at a time.

A temperature gradient across two dissimilar metal components of the IMP may be producing very small currents that get into the EUV-A detector signal current. Thus, as the IMP is warmed by the heater, a reverse current combined with the detector current makes the EUV-A net signal go down. When the heater goes off, the plates cool, and the current goes the other way, thus increasing the signal from the detector. Only the EUV optical housing that is mounted closest to the IMP seems to experience this heater noise, and within that housing, only the A channel is noticeably affected. In some of the EUVS sensors, the heater noise can also be seen in the B channel (mounted in the same housing) but this noise is vastly reduced and is therefore not removed from the signal.

The heater noise is partially removed from the GOES EUV-A data by using the SXI PCM2 temperature sensor as a proxy for the heater with a routine developed by R. Viereck. The SXI PCM2 temperatures are sampled about every 30 s. To process these data, the noise spikes and outliers are removed from the count data and then a 7 point or 3.5 minute box-car smoothing is applied. The first derivative of the temperature is then calculated. This first derivative looks similar to the heater noise in the EUV-A signal and is scaled to fit the EUV-A signal. A small time shift of the SXI PCM2 data is required to maximize the fit of the SXI PCM2 data to the EUV-A data but this shift and the scaling remain constant throughout the mission. An example of the Channel A data with the heater noise and the heater noise correction is shown in Figure 8.

The smoothing and the time-shifting of the SXI PCM2 data make it impossible to calculate the correction in real-time; however, the delay introduced by this process is less than 5 minutes. For GOES-15, the impact of the heater noise has not changed since launch. Heater noise corrections were done for GOES 13 and 15 only, because on GOES-14, there is SXI heater data only for 2009. On GOES 14, the A channel is expected to be much more impacted than the A' channel.

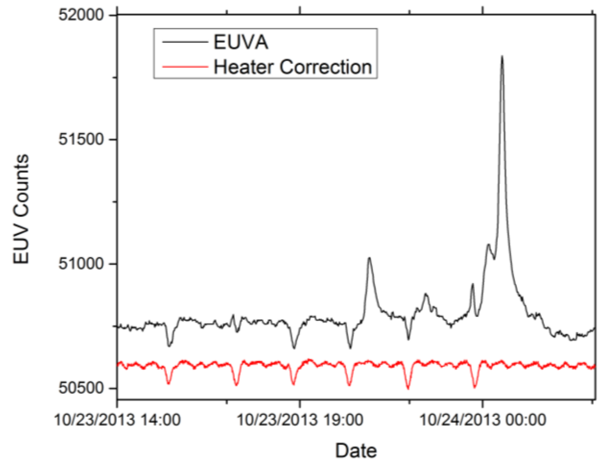

Figure 8. Channel A counts (black) showing heater noise and correction (red) based on SXI heater current.

B2. Calibrations

The original calibrations in the Handbook were done by ATC with the EUV beam at Brookhaven National Laboratory. The background values, *B*, do not vary much in time after the initial few months. We rederived these values by looking at measurements when the instrument was pointing away from the sun. We also rederived the conversion values, *C*, since the ones in the Handbook are of poor quality; they were created with a flat spectrum and are given in the wrong units --- [A/(W/m^2-nm)] instead of [A/(W/m^2)]. Previously, SWPC applied additional empirical correction factors in the conversion from counts to fluxes; these are no longer used.

Currently we do calibrations with quiet sun spectra. For the shorter wavelengths (channels A-D) we use the NRLEUV 2 updated Model Quiet Sun Irradiance Spectrum (Warren, 2005) and a flare spectrum (Meier et al., 2002) while for the Channel E around Lyman-α we use the LASP WHI quiet sun spectrum. Response curves for the channels A, B and E for GOES-15 are shown in Figure 9 through Figure 13 along with reference spectra for a quiet sun during solar minimum and maximum. The responses for the different satellites are similar but not identical.

More details such as impacts of solar activity, angle, particle backgrounds and limb effects could be considered. In the future, comparisons should be done for regimes based on solar activity, at least a quiet regime and a flare regime. Assuming solar maximum instead of solar minimum conditions can result in a 10% increase in the irradiance. However, when the bandpasses are scaled to match other instruments, sometimes the variability in f sometimes almost exactly cancels the variability in C, and so the net ratio between the instrument measurements does not change significantly.

For Channel E, a linear temperature dependent background resolved about half of the discrepancies with respect to SORCE SOLSTICE for GOES 15. For GOES 14, there are temperature variations up to 20 C in 2012 and a linear function was inadequate. Since the offpoint background measurements only cover a small temperature range, the background counts quadratic function from the Data Handbook was scaled to the measured background at 4.3 C, although this still does not adequately correct the data in 2012. It is not clear which other terms in Eq. 1 need to be calculated more carefully. Gain does not vary much with temperature and so the correction does not lie there. The visible light is missing a 3.4% 1 AU correction, but since the visible light is only about 1% of the total signal, this is also a very small effect. For GOES 13, which is misaligned to the sun, temperature and angular effects are known to be impacting the filter angle and require a more complicated correction [Viereck et al., 2007; Evans et al., 2010].

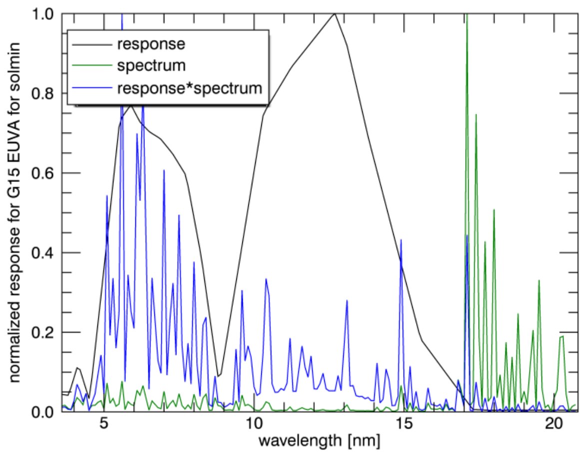

Figure 9. Response curve, solar minimum spectrum and response*spectrum for Channel A on GOES 15.

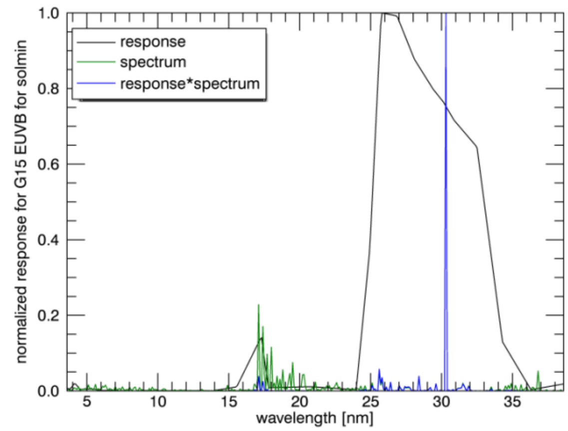

Figure 11. Same but for solar minimum for Channel B.

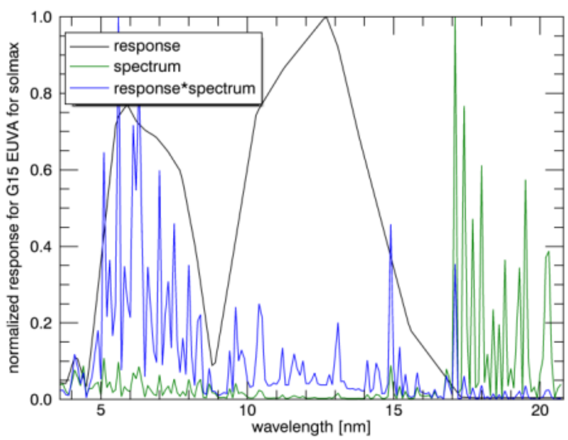

Figure 10. Same but for solar maximum for Channel A.

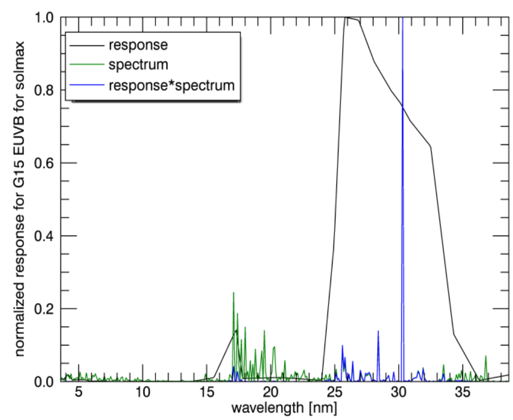

Figure 12. Same but for solar maximum for Channel B.

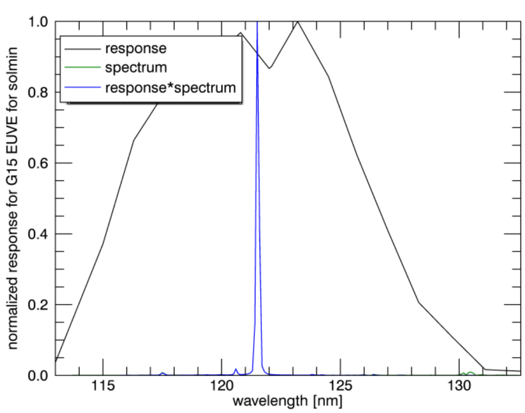

Figure 13. Same but for solar minimum for Channel E.

After applying a 1 AU correction to the data, it is compared with daily values from other instruments to test the calibrations. SDO EVE data was used for Channel A comparisons, SDO EVE and SOHO SEM data were used for Channel B, and SORCE SOLSTICE Lyman-α was used for Channel E comparisons. The equations for the calibrations are given below.

The photon irradiance values are given per 0.5 nm. Let's convert these to W m^{-2}. The resolution of 0.5 nm does not impact the equations; it is carried through.

The photon irradiance J_i are in units of [γ cm^{-2} s^{-1} $(0.5\ nm)^{-1}$]
The desired units are J_i[W m^{-2} $(0.5\ nm)^{-1}$].

E/photon= hc/λ[m] γ^{-1}= $hc/(\lambda[\text{nm}] \cdot 10^{-9}[\text{m/nm}])\ \gamma^{-1}$
with h=6.626x10^{-27} erg ·s, $c = 3 \times 10^8$ m s^{-1}, and 1 W= 10^7 erg s^{-1}

The conversion is then

$$J_i[\text{W m}^{-2}\ (0.5\ \text{nm})^{-1}] = J_i\ [\gamma\ \text{cm}^{-2}\ \text{s}^{-1}\ (0.5\ \text{nm})^{-1}] \cdot hc/(\lambda[\text{nm}] \cdot 10^{-9}[\text{m/nm}])\ \gamma^{-1}$$

$$= \frac{J_i\ [\gamma\ \text{cm}^{-2}\ \text{s}^{-1}\ (0.5\ \text{nm})^{-1}]\ \gamma^{-1} \cdot 10^{9}\ [\text{nm m}^{-1}] \cdot (6.626\text{x}10^{-27}\ \text{erg} \cdot \text{s} \cdot 3 \times 10^{8}\ \text{m s}^{-1})\ (1\text{W} \cdot 10^{-7}\ \text{erg}^{-1}\ \text{s}) \cdot [10^{4}\ \text{cm}^{2} \cdot \text{m}^{-2}]}{\lambda[\text{nm}]}$$

$$= \frac{J_i\ [\text{cm}^{-2}\ \text{s}^{-1}\ (0.5\ \text{nm})^{-1}] \cdot 1.988\text{x}10^{-12}\ [(\text{cm}^{2}\ \text{s nm})\ (\text{W m}^{-2})]}{\lambda[\text{nm}]}$$

For the quiet regime, the total irradiance over the band is given by

$$J_{tot\_quiet}\ [W\ m^{-2}] = \sum_i J_i[\text{W m}^{-2}\ (0.5\ \text{nm})^{-1}]$$

The current for the quiet time is given by

$$I_{tot\_quiet}[A] = \sum_i\ R_i[A\ m^2\ W^{-1}]\ \cdot\ J_i[\text{W}\ m^2\ (0.5\ \text{nm})^{-1}]$$

So now, if we measure a current, I_{meas}, during a quiet time, then the total flux in the band is

$$J_{tot\_meas} = (J_{tot\_quiet} / I_{tot\_quiet}) \cdot I_{meas}$$

To compare with another instrument on a different type of satellite, we scale the total flux by the fraction of the flux that is in the bandpass of the other instrument. We can also estimate the fraction of irradiance in energy units in some band subset with

$$f_{subset} = \sum_i J_i[\text{W m}^{-2}\ (0.5\ \text{nm})^{-1}]\ /\ J_{tot\_quiet}\ [W\ m^{-2}]$$ where i is in subset

Appendix C. Comparisons with other satellite data

This section shows time series of GOES irradiances as well as comparisons with the following calibrated data sets: SDO EVE, version 4; SOHO SEM, version 3; and SORCE SOLSTICE Lyman-α, version 15. To compare the irradiance for the GOES Channels A and B with irradiance from another satellite instrument we estimated the fraction of the GOES channel irradiance that would fall in the other instrument bandpass as described in Appendix B4. The GOES data was adjusted to 1 AU for the comparisons with the other data sets. The SOHO SEM data has 17-nm scatter into this band which sometimes results in a double-humped peak for each solar rotation since it is has an angular factor (A. Jones, personal communication). Major sources of discrepancies between data sets are calibration errors, incomplete correction for differing bandpasses, and the use in the GOES calibrations of solar minimum reference factors instead of factors that vary with solar activity.

C.1 Channel A

C.1.1 GOES-15

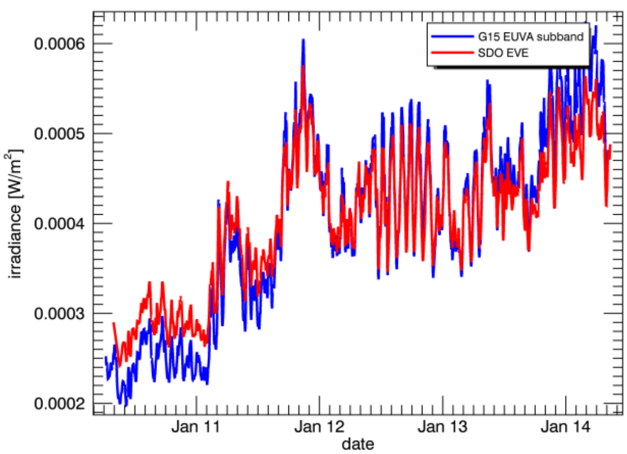

Figure 14. Comparison of the EVE MEGSA 'GOES-A' band with the 5-15 nm subset of the GOES-15 Channel A.

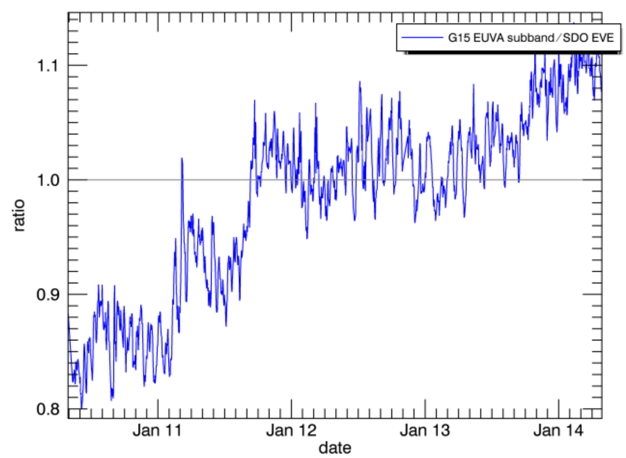

Figure 15. Ratio of GOES-15 EUV-A to EVE GOES-A band.

C.1.2 GOES-14 Channels A and A'

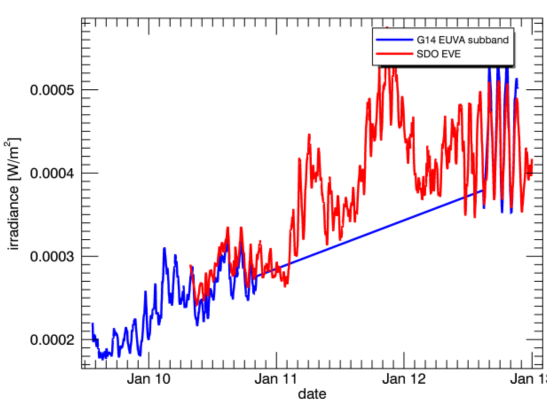

Figure 16. Comparison of the EVE GOES-A band (derived from MEGS A for the 5 to 15 nm band) with a subset of the GOES-14 Channel A data from 5-15 nm.

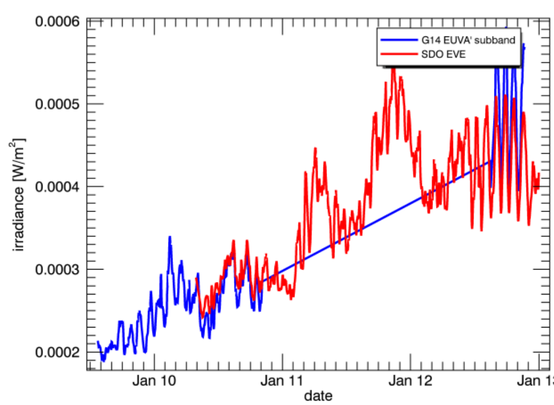

Figure 17. Comparison of the EVE GOES-A band (derived from MEGS A for the 5 to 15 nm band) with a subset of the GOES-14 Channel A' data from 5-15 nm.

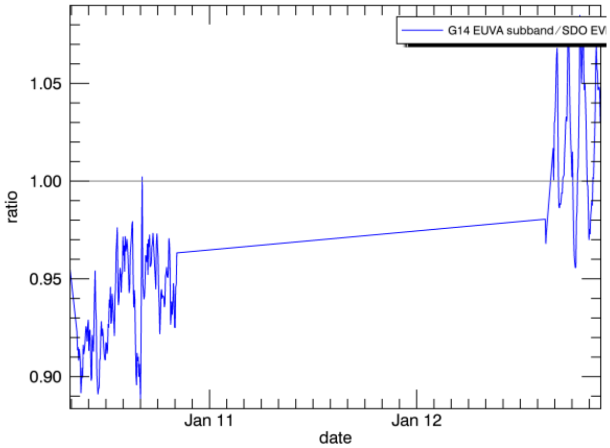

Figure 18. Ratio of GOES-14 EUV-A to EVE GOES-A band.

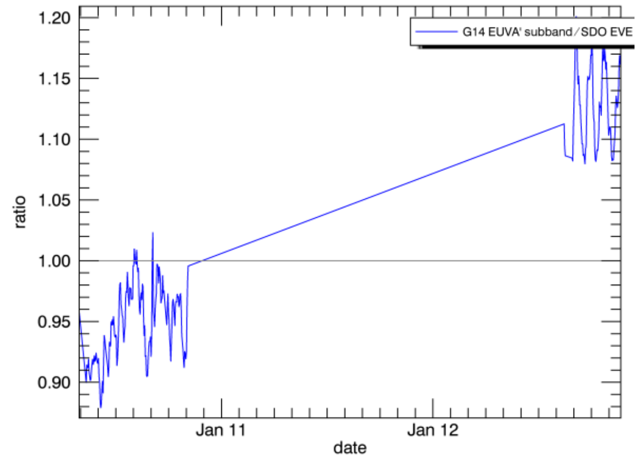

Figure 19. Ratio of GOES-14 EUV-A' to EVE GOES-A band.

C.1.3 GOES-13 Channel A

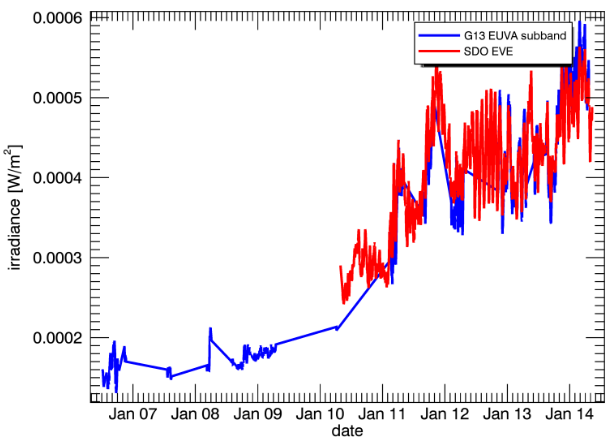

Figure 20. Comparison of the EVE GOES-A band (derived from MEGS A for the 5 to 15 nm band) with a subset of the GOES-13 Channel A data from 5-15 nm.

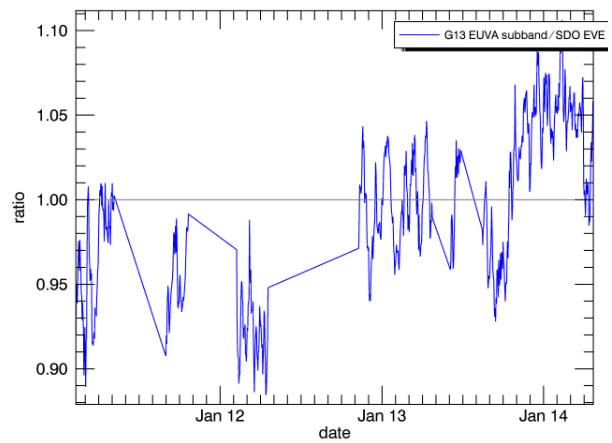

Figure 21. Ratio of GOES-13 EUV-A to EVE GOES-A band.

C.2 Channel B

C.2.1 GOES-15 Channel B

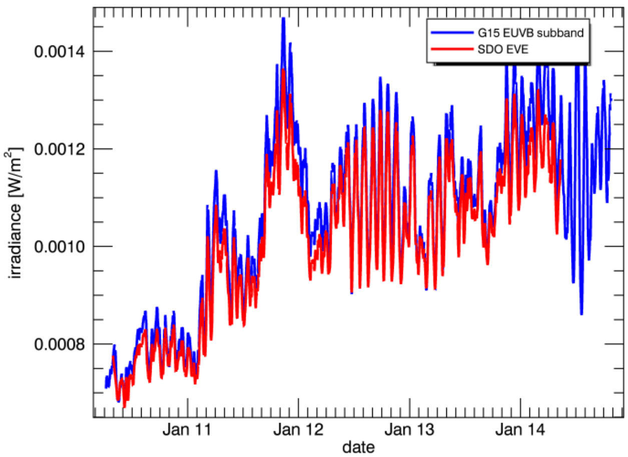

Figure 22. Comparison of the 25-34 nm subset of the GOES-15 Channel B data with the EVE 'GOES-B' band.

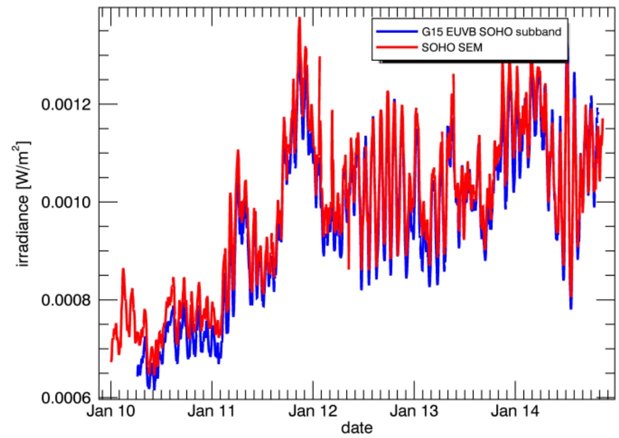

Figure 23. Comparison of the 26-34 nm subset of the GOES-15 Channel B data with the SOHO SEM 26-34 nm band.

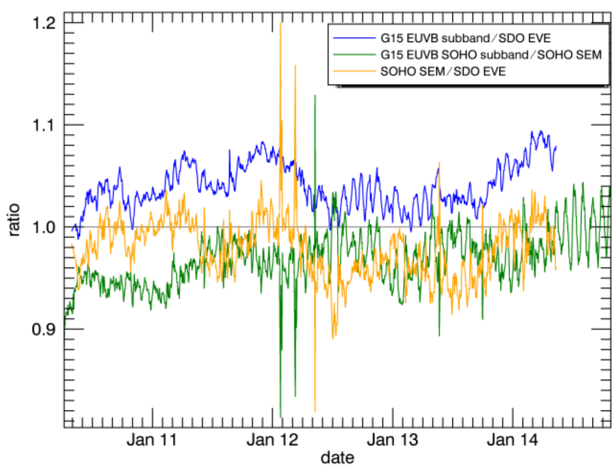

Figure 24. Ratios between GOES 15 EUVS-B, SDO EVE, and SOHO SEM

C.2.2 GOES-14 Channels B and B'

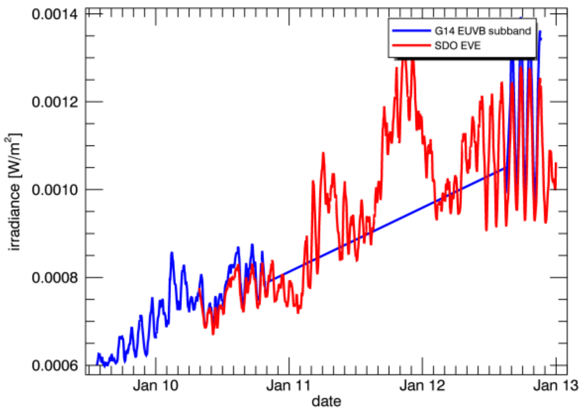

Figure 25. Comparison of the EVE GOES-B' band with subset of the GOES-14 Channel B data from 25-34 nm.

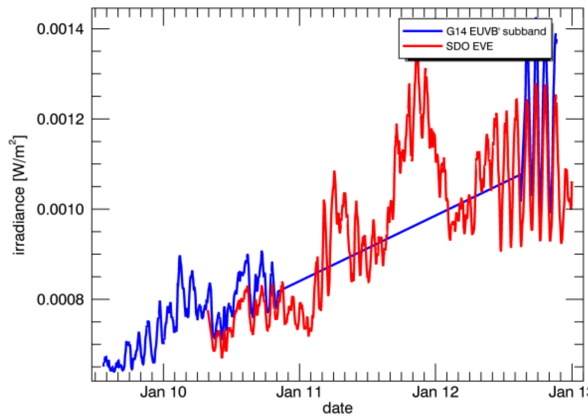

Figure 26. Comparison of the EVE 'GOES-B' band with subset of the GOES-14 Channel B' data from 25-34 nm.

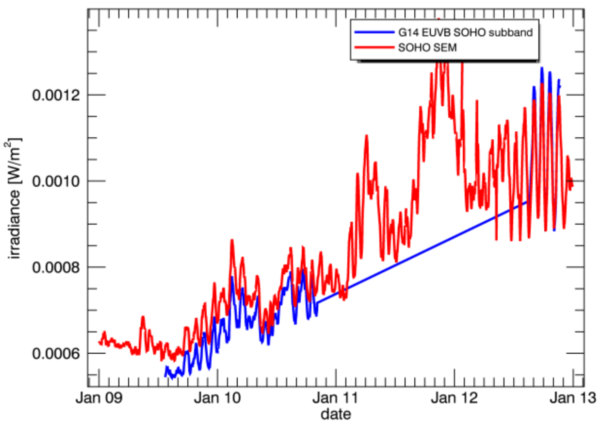

Figure 27. Comparison of the SOHO SEM 26-34 nm band with subset of the GOES-14 Channel B data from 26-34 nm.

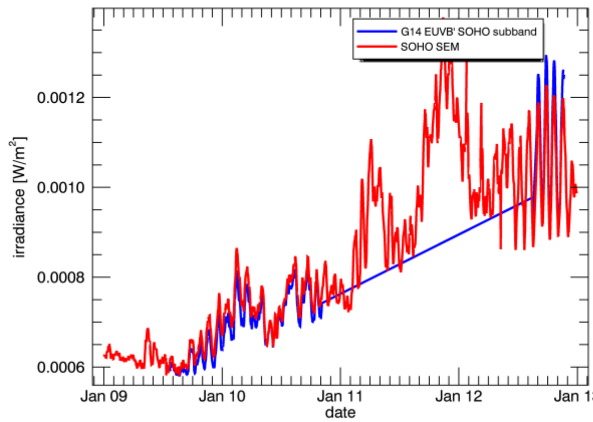

Figure 28. Comparison of the SOHO SEM 26-34 nm band with subset of the GOES-14 Channel B' data from 26-34 nm.

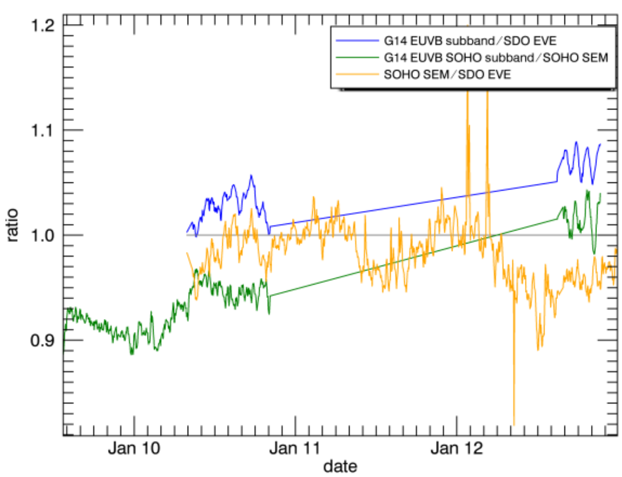

Figure 29. Ratios between GOES 14 EUVS-B, SDO EVE, and SOHO SEM.

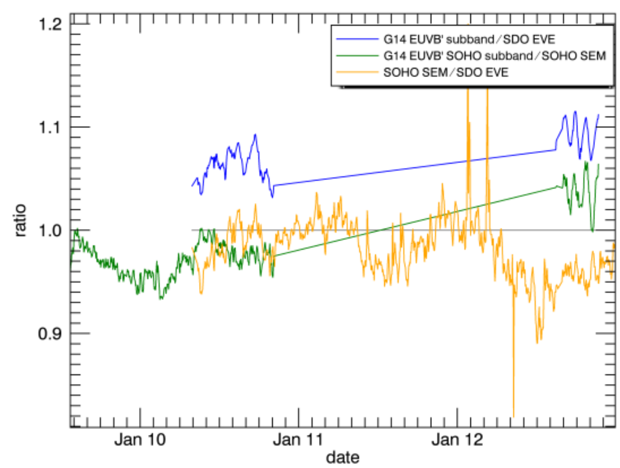

Figure 30. Ratios between GOES 14 EUVS-B', SDO EVE, and SOHO SEM.

C.2.3 GOES-13 Channel B

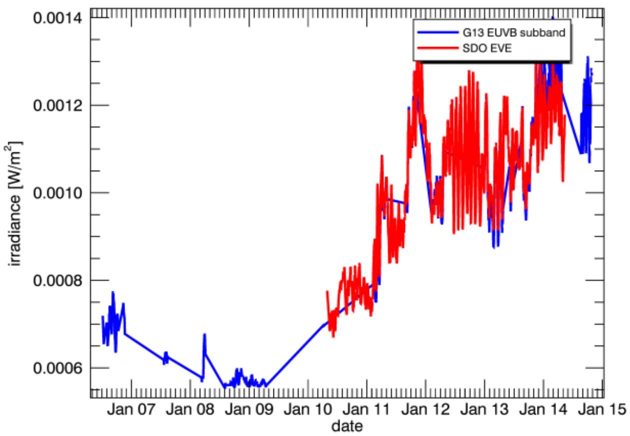

Figure 31. Comparison of the EVE 'GOES-B' band with subset of the GOES-13 Channel B data from 25-34 nm.

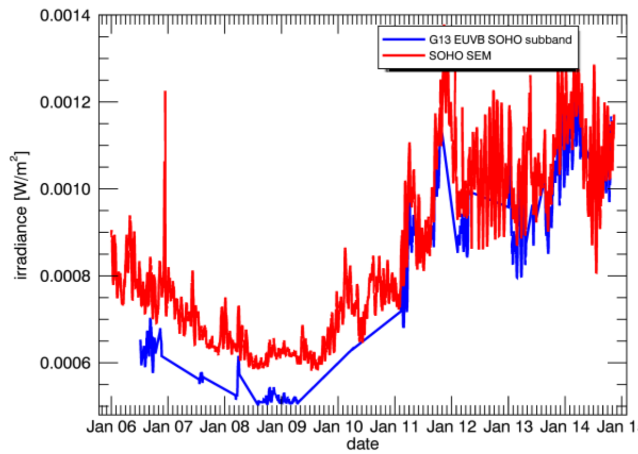

Figure 32. Comparison of the SOHO SEM 26-34 nm band with 26-34 nm subset of the GOES-13 Channel B data.

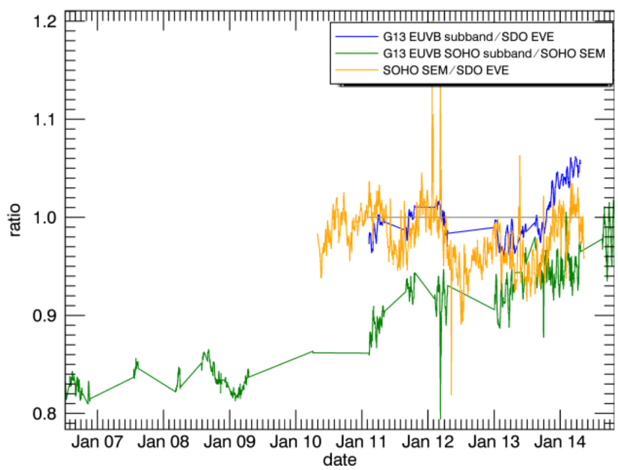

Figure 33. Ratios between GOES 13 EUVS-B, SDO EVE, and SOHO SEM.

C.3 Channel E

C.3.1 SORCE SOLSTICE Lyman-alpha v15

The GOES Ch E data is scaled to the SORCE SOLSTICE Lyman-alpha v15 data shown in Figure 34.

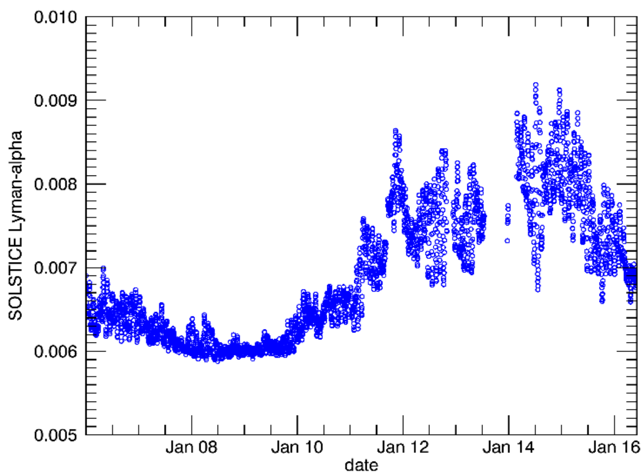

Figure 34. Daily SORCE SOLSTICE measurements of irradiance in the 1 nm band over Lyman-alpha.

C.3.2 GOES-15 Channel E

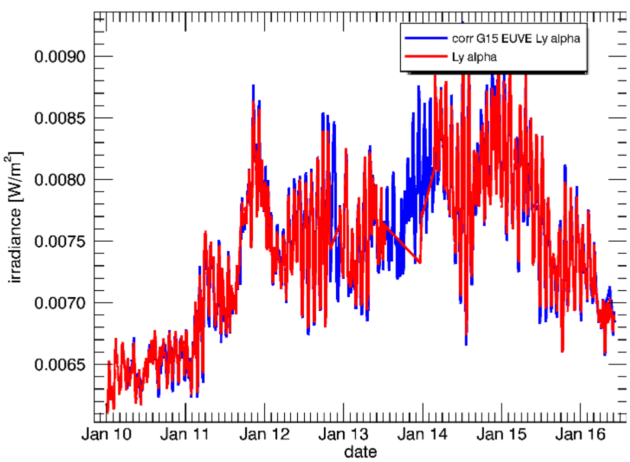

Figure 35. Comparison of the scaled and degradation-corrected GOES-15 Channel E data from 121.0-121.0 nm to the SORCE SOLSTICE Lyman-α.

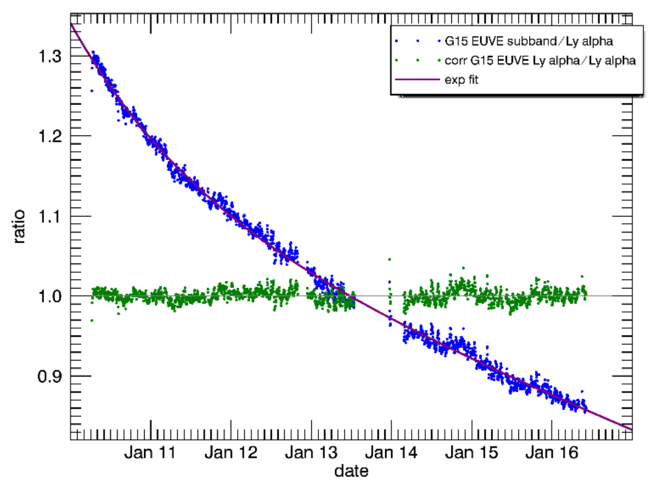

Figure 36. Ratio of GOES-15 EUVS-E to the SOLSTICE elements of the SORCE SOLSTICE Lyman-α (blue dots). The ratio is fit (purple line). This fit is used both to determine the decay rate and to correct the data. The residual (green dots) is <±2%.

C.3.3 GOES-14 Channel E

The Channel E measurements prior to 1 Dec 2009 has a much slow decay and the reason for this is not known, and so the degradation fit is started on that date. Flags are set to 1 for the early time period to note that it has a questionable calibration.

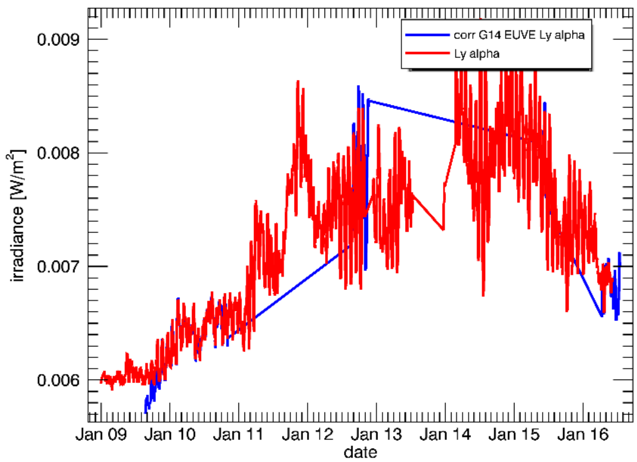

Figure 37. Comparison of the scaled and degradation-corrected GOES-14 Channel E data from 121.0-121.0 nm to the SORCE SOLSTICE Lyman-α.

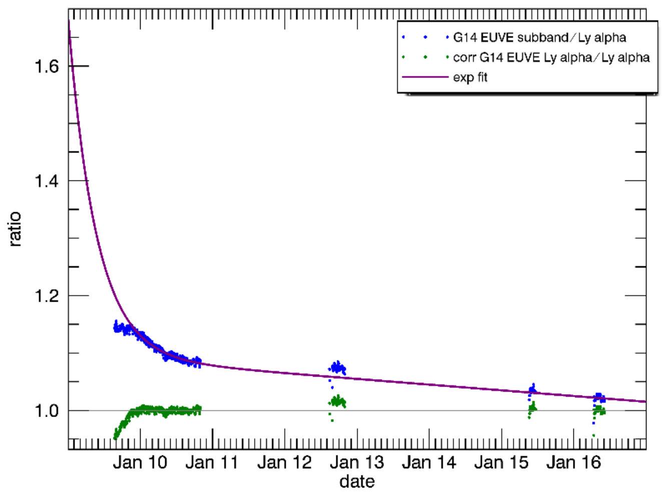

Figure 38. Ratio of GOES-14 EUVS-E to the SOLSTICE elements of the SORCE SOLSTICE Lyman-α (blue). The fit (purple) and residual (green) are shown.

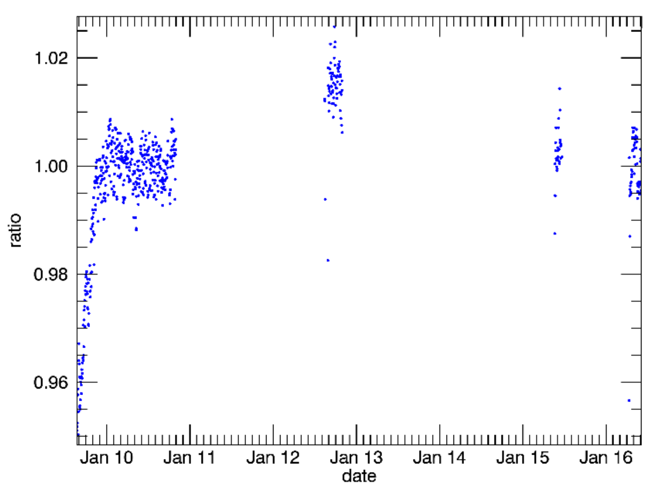

Figure 39. Residual of ratio shown in Figure 38.

C.3.4 GOES-13 Channel E

More work needs to be done to correct the GOES-13 Channel E data and this data should not be used.

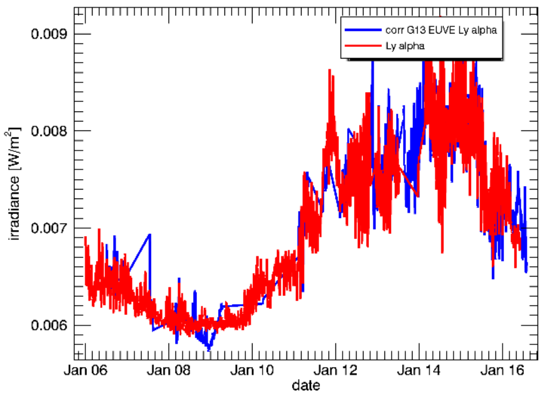

Figure 40. Comparison of the scaled and degradation-corrected GOES-13 Channel E data from 121.0-121.0 nm to the SORCE SOLSTICE Lyman-α.

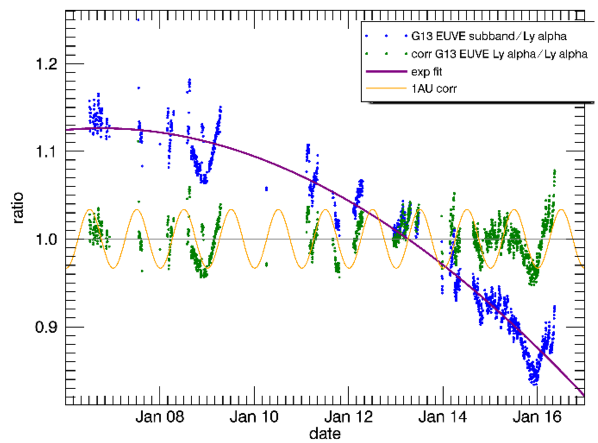

Figure 41. Ratio of GOES-13 EUVS-E to the SOLSTICE elements of the LASP Lyman-α Composite (blue dots). The ratio is fit with a function (purple line). The 1AU correction is shown as a guide to the eye for possible future seasonal temperature and angle corrections.

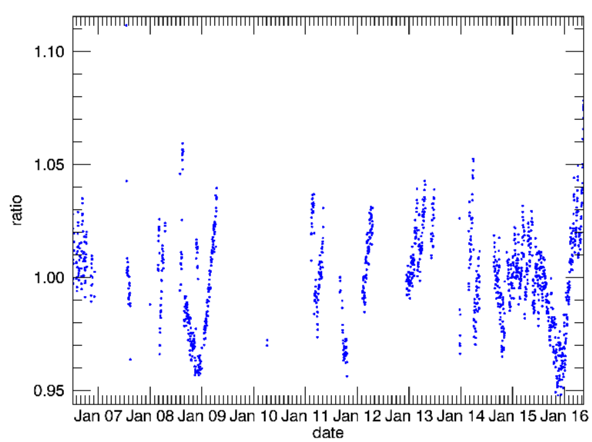

Figure 42. Residual of ratio shown in Figure 41.

Appendix D. GOES EUVS hardware

The EUVS on GOES-13-15 were all very similar. The five channels of the EUV were measured via three spectrograph units with east-west dispersion. The units vary in the grating spacing, For GOES 13 and 15, the first unit measure channels A and B and the second unit measures channel s C and D. For GOES 14, the first unit measures channels A and B, and the second unit measures channels A' and B'. The measurements are redundant except that the A'-B' detectors are arranged in opposite order so that they have opposite impacts of angular effects from sources near the solar limb. The intent is that each pair of channels can be averaged to produce an irradiance with reduced error due to angular effects. For all three GOES satellites, Channel E is measured on a separate spectrograph. Sample rates are once every 32.768 s. Table 14 shows some details of the spectrograph elements, specifically the hardware design, manufacturer, components, contamination and degradation.

Table 14. Hardware components for EUVS on GOES 13-15. Note that on GOES-14, the C and D channels are at the usual A and B wavelengths.

instrument/component	manufacturer	details
EUVS	ATC	There are 3 optical benches: one for A and B, one for C and D (or A' and B' on GOES-14), and one for E. Nominal wavelengths (nm) are: A: 5-15, B: 25-34, C: 17-67, D: 17-84, E: 118-127
detectors	IRD	AXUV photodiode On GOES-14,channels B, B' and E are nitrided.
gratings	MIT	A,B: 5000 lines/mm C,D: 2500 lines/mm E: 1667 lines/mm
thin film filters on detectors	Lebow	A: 50/200/70 nm of Ti/Mo/C B: 150/5 nm of Al/Al_2O_3 C: 150/2 nm of Al/Al_2O_3 D: 150/2 nm of Al/Al_2O_3
Lyman-α filter	Acton Labs	free standing

Several design features and manufacturing techniques were incorporated to minimize the impact of contamination (Viereck et al., 2007). The first optical component is the transmission grating. The buildup of contaminants from outside the sensor will occur primarily on the grating bars which will have minimal impact on the transmission properties. The grating can accumulate 10's of nm of molecular contaminants before experiencing a noticeable change in transmission whereas an optical component such as a filter or window will exhibit a significant decrease in performance (depending on the material) for more than about 0.5 nm of contaminants. To minimize the contaminants on internal optical surfaces, the EUVS was manufactured in a clean environment. The few electronic components and wires required to control and read the silicon diodes are at the back of the optical housing and are kept extremely clean. The entire package was stored with a dry nitrogen purge or in a vacuum during most of its testing and prelaunch storage activities. Zeolite absorbers inside the optical housing are designed to capture any residual contaminants that remain inside the optical housing after launch.